Ecological Engineering 170 (2021) 106354

Contents lists available at ScienceDirect

Ecological Engineering

journal homepage: www.elsevier.com/locate/ecoleng

On the use of large-scale biodegradable artificial reefs for intertidal foreshore stabilization

Beatriz Marin-Diaz [a,b,*], Gregory S. Fivash [a], Janne Nauta [b], Ralph J.M. Temmink [c], Nadia Hijner [b], Valérie C. Reijers [i,d], Peter P.M.J.M. Cruijsen [c], Karin Didderen [e], Jannes H. T. Heusinkveld [f], Emma Penning [a], Gabriela Maldonado-Garcia [a,f], Jim van Belzen [a], Jaco C. de Smit [a], Marjolijn J.A. Christianen [g,c], Tjisse van der Heide [d,b,c], Daphne van der Wal [a,h], Han Olff [b], Tjeerd J. Bouma [a,b,i], Laura L. Govers [b,d]

[a] NIOZ Royal Netherlands Institute for Sea Research, Department of Estuarine and Delta Systems, PO Box 140, 4400 AC Yerseke, the Netherlands
[b] Conservation Ecology Group, Groningen Institute for Evolutionary Life Sciences, University of Groningen, PO Box 11103, 9700 CC Groningen, the Netherlands
[c] Aquatic Ecology and Environmental Biology, Institute for Water and Wetland Research, Radboud University, Heyendaalseweg 135, 6525 AJ Nijmegen, the Netherlands
[d] Department of Coastal Systems, NIOZ Royal Netherlands Institute of Sea Research, PO Box 59, 1790 AB Den Burg, the Netherlands
[e] Bureau Waardenburg, Varkensmarkt 9, 4101 CK Culemborg, the Netherlands
[f] The Fieldwork Company, Groningen, the Netherlands
[g] Wageningen University & Research, Aquatic Ecology and Water Quality Management Group, P.O. Box 47, 6700 AA Wageningen, the Netherlands
[h] Faculty of Geo-Information Science and Earth Observation (ITC), University of Twente, PO Box 217, 7500 AE Enschede, the Netherlands
[i] Department of Physical Geography, Faculty of Geosciences, Utrecht University, PO Box 80115, 3508 TC Utrecht, the Netherlands

ARTICLE INFO

Keywords:
Coastal protection
Ecosystem-based coastal defence
Ecosystem connectivity
Ecosystem restoration
Sediment dynamics
Wave attenuation

ABSTRACT

Combining foreshore ecosystems like saltmarshes and mangroves with traditional hard engineering structures may offer a more sustainable solution to coastal protection than engineering structures alone. However, foreshore ecosystems, are rapidly degrading on a global scale due to human activities and climate change. Marsh-edges could be protected by using connected ecosystems, such as shellfish reefs and seagrass beds, which can trap and stabilize sediments, thereby reducing hydrodynamics loads on the saltmarsh edge. In our study, we aimed to test the effect of large-scale biodegradable artificial reefs on tidal flat accretion and/or stabilization. We hypothesized that the structures would attenuate waves and trap sediment. For this, a large-scale experiment was conducted on the tidal flats of the Dutch Wadden Sea, by installing biodegradable artificial reefs along 630 m. Waves, sediment dynamics and sediment properties around the structures were monitored over three years. Our results demonstrate that intact structures attenuated circa 30% of the wave height with water levels below 0.5 m. Variability in wave-attenuation increased when the wind direction was parallel to the structures/foreshore. Sediment dynamics were variable due to the exposed nature of the location and environmental heterogeneity because of the landscape-scale set-up. We observed local sediment accretion up to 11 cm, however the effect did not expand beyond 10 m from the landward edge of the structures and up to 10 cm scouring was also found. Additionally, near sediment properties were not affected by the presence of the artificial reefs. Long-term effects could not be assessed due to the degradation of the structures during the experimental period. In general, we conclude that artificial reefs have the potential to attenuate waves and trap sediment on tidal flats. However, to benefit connected foreshore ecosystems like salt marshes, an even larger implementation scale and the use of more resistant structures in exposed sites is needed to affect long-term tidal flat morphology.

1. Introduction

Combining natural ecosystems, such as saltmarshes and mangroves, with hard engineering structures, such as sea walls and dikes, may enhance coastal flood protection compared to hard engineering alone, while simultaneously improving the foreshore ecosystem and its linked

* Corresponding author at: NIOZ Royal Netherlands Institute for Sea Research, Department of Estuarine and Delta Systems, PO Box 140, 4400 AC Yerseke, the Netherlands.
E-mail address: b.marin.diaz@rug.nl (B. Marin-Diaz).

https://doi.org/10.1016/j.ecoleng.2021.106354
Received 27 January 2021; Received in revised form 15 June 2021; Accepted 27 June 2021
Available online 24 July 2021

services (Temmerman et al., 2013; Schoonees et al., 2019). These foreshore ecosystems are able to attenuate waves (Barbier et al., 2011; Shepard et al., 2011), even under extreme storm surge conditions (Möller et al., 2014; Willemsen et al., 2020). Moreover, historic data demonstrated that marshes in front of a dike both reduce the chance of dike breaching during extreme events, and the size of dike breaches when dikes fails (Zhu et al., 2020). To be able to rely on natural ecosystems, such as saltmarshes and mangroves, for flood defence, their width must be persistent and predictable over time (Bouma et al., 2014). Ecosystems located in the lower intertidal, such as mussel beds or seagrass meadows, may facilitate the stability of protective natural ecosystems, such as salt marshes and mangroves (Gillis et al., 2014; van de Koppel et al., 2015). However, as these ecosystems located lower in the intertidal zone attenuate waves less effectively than upper intertidal salt marshes and mangroves (Bouma et al., 2014), they are often neglected.

The morphology of tidal flats is important for the stability of the edges of marshes and mangrove forests. Several recent studies show that higher, wider, convex and gentler sloping tidal flat profiles may attenuate waves more efficiently. This leads to reduced erosion in the pioneer vegetation zone of a salt marsh (Mariotti and Fagherazzi, 2013; Hu et al., 2015; Bouma et al., 2016; Willemsen et al., 2017). In this context, oyster and mussels beds that occur much lower in the intertidal than salt marshes, may be efficient in protecting the marsh edge from eroding by attenuating waves and inducing accreting conditions (Meyer et al., 1997; Borsje et al., 2011; Donker et al., 2013; Walles et al., 2015). Seagrass beds can also attenuate waves and stabilize the sediment, and may therefore also improve stability and morphology of tidal flats (Fonseca and Cahalan, 1992; Bos et al., 2007; Christianen et al., 2013; Marin-Diaz et al., 2019).

To date, many natural foreshore ecosystems are degrading due to sea level rise, changes in sediment supply, eutrophication, overexploitation and ocean sprawl among others (Bishop et al., 2017; Ladd et al., 2019; Murray et al., 2019). Additionally, landward migration of foreshore ecosystems to keep pace with sea level rise is often prevented due to the presence of dikes and sea walls (Doody, 2013). As a result, coastal ecosystems are steepening, thereby making protective natural ecosystems, such as salt marshes and mangroves more prone to edge erosion, and lowering benefits from physical facilitation by lower intertidal ecosystems. In such situations, foreshore erosion is typically reduced by using hard-engineered coastal structures such as groynes and breakwaters (Schoonees et al., 2019; Siemes et al., 2020), stone dams (Van Loon-steensma and Slim, 2013) or concrete reefs (Chowdhury et al., 2019). Trials of more environmentally friendly options, such as the restoration of biogenic reefs (e.g. dominated by oysters or mussels) at a large scale and at exposed sites remain scarce (Bouma et al., 2014; Morris et al., 2018), and their success is often negatively affected by the strong hydrodynamics (De Paoli et al., 2015; Schotanus et al., 2020).

BESE-biodegradable artificial reef-structures (https://www.bese-products.com), have been shown to be suitable for restoring mussel beds, seagrass and marsh vegetation at small scales (Fivash et al., 2020; Temmink, 2020; Temmink et al., 2020). In addition having such hard structures in the tidal flat could change the tidal flat morphology, which ultimately could be beneficial for adjacent saltmarsh stability. In this study, we aimed to test how the use of these biodegradable artificial reef-structures at a larger scale would 1) attenuate waves, 2) change tidal flat morphology, and 3) affect the near surrounding sediment properties. We hypothesized that artificial reef structures would promote sediment accretion, but that long-term morphological effect of these structures would depend on their structural integrity. For this, we set up a large-scale experiment on the tidal flats of the Dutch Wadden Sea, consisting of BESE-biodegradable artificial reef-structures along 630 m, which also provided hard substrate for mussel settlement (Temmink et al., 2020).

2. Methods

2.1. Study site

The Wadden Sea is a very extensive intertidal flat system listed as UNESCO World Heritage since 2009 and part of the Natura 2000 protected areas in Europe. This shallow inland sea stretches for ~500 km along the coast of the Netherlands, Germany and Denmark. Natural reefs of blue mussel (*Mytilus edulis*), which declined in the 1990 due to overfishing and are slowly recovering, and Pacific oyster (*Crassostrea gigas*), which was introduced in 1960, do occur in this area (Christianen et al., 2017; Folmer et al., 2017). The field experiment was conducted on an exposed intertidal area south of Griend, a fetch-limited island in the Dutch Wadden Sea (53°14′24.97″N, 5°14′53.56″E) (Fig. 1a). The tidal flat is sandy and long straight bedforms of approximately 2 to 6 cm high and 10 to 30 m width can be observed on the flat (Fig. 1b and A. 3). In this area, the normal tidal range is ~190 cm (RWS, 2013). Wind direction and wind speed during the experimental period were obtained from the Royal Dutch Meteorological Institute (KNMI), recorded in the weather station of Vlieland, at ~11 km from Griend (53°17′49.4″N 5°05′27.6″E).

2.2. Study design and deployment of the artificial-reef structures

The experimental set-up consisted of sixteen plots installed perpendicular to the nearest gully at a mean elevation of −0.32 ± 0.003 m NAP (Dutch ordinance level, close to the Dutch mean sea level) and a mean inundation frequency of 65% (Fig. 1b). Plots were grouped in blocks (n = 4 blocks) with plots randomly assigned to either i) unmodified control (from here on called 'Control') or ii) artificial reef treatment (from here on called 'Reef'). Each artificial reef plot consisted of ten bands of 5 m long, each one made of 5 modules which consisted of 8 layers of stacked biodegradable BESE-sheets of 91.5 × 45.5 × 2 cm (L × W × H) (Fig. 1c). The BESE is made from biodegradable potato-waste derived Solanyl C1104M (Rodenburg Biopolymers, Oosterhout, the Netherlands). Each module was braided with 70 m of coir rope and placed on anti-erosion coir mats (~4 cm thick) and secured with 1.5 m long L-shaped anchors. Once the modules were installed, the height of the artificial reefs was ~20 cm above the bed level. In total, the plots measured 20 × 10 m (Fig. 1c). Control plots were completely bare and unmodified (Fig. 1d). The reef structures were deployed in March of 2017 and monitoring was conducted in May 2017, August 2017, August 2018 and August 2019 (Fig. 1e).

2.3. Wave measurements and data analyses

Four pressure sensors (wave loggers, OSSI-10-003C) were deployed 10 cm above the bed level in the artificial reef plot R9 and the control plot C10, which were randomly selected, to monitor the effect of the artificial reef on wave dampening. We assumed similar effects for the other reefs, which were all located in the same orientation (340°) and tidal elevation. The reference sensor was located −5 m seaward between the plot R9 and C10 (Fig. 1d). Two other sensors were located in the plot R9 in between the artificial reef (+1.7 m) and + 10 m landward from the artificial reef and one sensor in the control C10 at the same distance as the sensor at +10 m from the artificial reef. Data was recorded between March 2017 to August 2017 (period 1), September 2017 to January 2018 (period 2) and January 2019 to March 2019 (period 3) (Fig. 1e). These periods were categorized based on the wave logger deployment and measurements of the degradation of the structures. Unfortunately, the sensor in the control plot got lost as a result of ice-sheet formation on the tidal flat in March 2018. Therefore, the analysis of period 2 and 3 only include the sensors in the artificial reef plot.

Data was recorded with a 7-min interval every 15 min with a measuring frequency of 10 Hz. For every sensor, significant wave height (H_s) was determined through spectral analysis of the wave time series

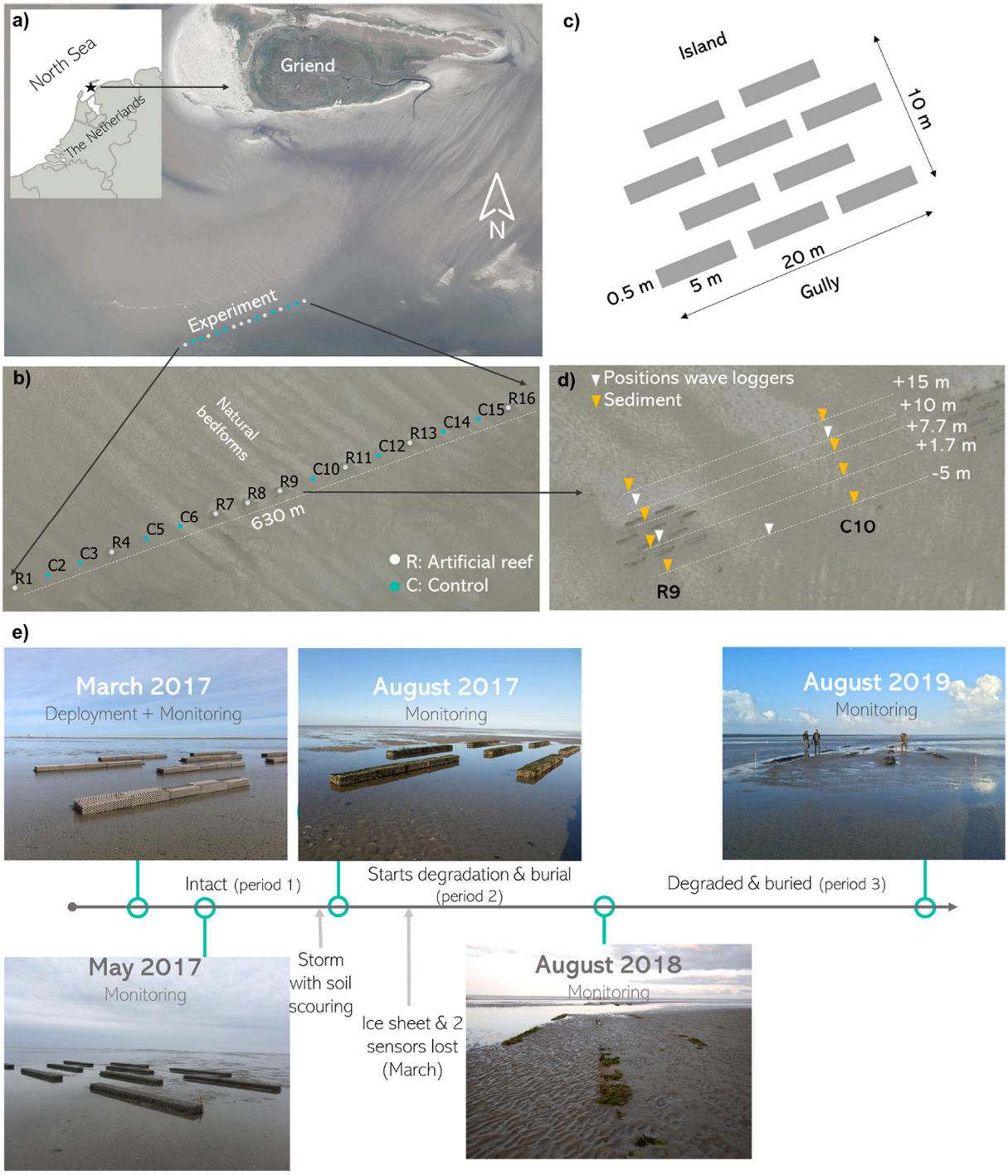

Fig. 1. a) Location of the experiment in the southern tidal flat of Griend, b) plots of the experiment and view of the large bedforms in 2017, c) set-up of an artificial reef plot consisting of 10 bands, d) position of the wave loggers in plot number 9 (artificial reef) and plot number 10 (control) and the distances where sediment samples were collected; and e) timeline of the experiment and degradation of the structures.

after correcting for air pressure (Appendix A). To reduce stochasticity in the wave attenuation analysis, records with $H_s < 0.05$ m (too small), $H_s/h < 0.2$ (waves too small relative to the water level) and $H_s/h > 0.4$ (higher probability of breaking waves) were excluded (Kroon, 1994; Donker et al., 2013). H_s was then split into tidal cycles and categorized into rising or falling tide. H_s and mean water depth during the highest point of the tides, considered stable sea state, were used to relate to wind conditions. Wave attenuation was calculated as the percentage of H_s reduction between the reference sensor and the sensors in the artificial reef R9 and control C10.

2.4. Bed level change and reef degradation

Tidal flat elevation was monitored along 5 evenly-spaced transects of 105 m long in each plot via rtk-dGPS. The transect started −5 m seaward from the artificial reefs and finished 100 m landwards of the reefs. The vertical resolution was 1 mm. Horizontally, the interval of measurements was 10 m at the large scale and 1 m at the local scale. These measurements were taken in March 2017 (only the central transect per plot), May 2017, August 2017 (not all the plots completed), August 2018 and August 2019. Digital elevation models (DEM) were created with a

grid cell of 10 cm for each time-step by interpolating the dGPS points using the natural neighbour method from QGIS software. Elevation change was calculated at a large scale (plots of 20 × 105 m) and at local scale (reef section of 20 × 10 m) by subtracting each time-step DEM from the initial DEM from March 2017. Estimation of the artificial reef height degradation over time was calculated as the difference in the reef elevation for each time-step compared to March 2017. The artificial reef elevation was measured in the central transect of each plot by placing the dGPS on the top of the artificial reef.

2.5. Sediment properties

To investigate the effect of the artificial reefs on the edaphic conditions over time, sediment properties were determined across the central transect at positions −5, +1.7, +7.7 and +15 m in the 12 most westward plots (1 to 12, $n = 6$ for each treatment) (Fig. 1d). Sediment properties were determined from samples of the top 5 cm of sediment, collected with a 3 cm Ø core. Sediment samples were freeze dried during four days and sieved with a 0.8 mm mesh. Grain size was determined for all time steps using a Malvern® Mastersizer 2000. Organic matter content was determined by weight loss on ignition (LOI, 4 h at 550 °C) during all monitoring campaign until August 2018.

2.6. Statistical analyses

Relationships between wave attenuation and water depth were explored with Spearman's rank correlations. Two-way ANCOVAs were used to test differences on slopes of wave attenuation between i) the control plot and artificial reef plot (inside the reef and + 10 m landward from the reef) and ii) rising and dropping tide, with mean water depth as a covariate (i.e. slopes were considered different when the interaction between treatment and water depth was significant). To further test the effect of wave attenuation by the reef at different water depths during period 1, the water depth was categorized into 3 groups (form 0.15 to 0.3, 0.3 to 45 and 0.45 to 0.6 m water depth). Two-way ANOVAs were performed with treatment and water level as factors and wave attenuation as response variable, followed by Tukey post hoc test for i) data including all the wind directions to have an overall effect, ii) data only including wind directions coming perpendicular to the set-up to avoid possible confounding effects due to the wind direction (i.e. both control and reef were subjected to the same waves coming offshore). Differences in i) maximum sediment accretion per plot and ii) maximum erosion per plot, iii) standard deviation of the accretion per plot and iv) net sediment accretion per plot, between control and artificial reef plots were analysed with a 3-way ANOVA including block and time. Tukey HSD post-hoc tests were used to distinguish significant differences between groups. Linear mixed models were used to study the main and interactive effects of the artificial reefs, time and position on the transect on sediment grain size and sediment organic content, with block as random effect. The significance of the fixed factors was tested with the Type II Wald Chi-square test. Assumptions of normality and homogeneity of variance were analysed with histograms and residual plots. Wave attenuation, when including all the wind directions, contained several outliers and was cube root transformed, and in addition to the two-way ANOVA, Kruskal-Wallis non-parametric tests were performed to confirm the results. All statistical analyses were performed using R 3.5.0 (R Development Core Team 2018). The lme4 package (Bates et al., 2015) was used for the linear mixed models.

3. Results

3.1. Wave attenuation and reef height reduction over time

The artificial reef structures were still intact in May 2017 and August 2017. The differences in the SD likely came from measurement error in the field. In August 2018, after a winter with heavy storms and abrasion by ice sheet formation, the artificial reefs lost around 12 cm of height. This was around 50% of the initial elevation. In August 2019, the artificial reefs lost another 2 cm, which left a reef of circa 6 cm height (Table 1, Fig. 2e).

From March 2017 to August 2017, the artificial reef, either inside and + 10 m landward, attenuated significant wave heights on average by 30%, reaching a maximum of 60%, when compared to the bare plot, including all the wind directions (Fig. 2a). The amount of wave attenuation was dependent on the water depth (ANCOVA for period 1: $F_{2,519} = 7.1$, $p < 0.001$) (Fig. 2a). There were no significant effects in attenuation during the rising or dropping tide (ANCOVA for period 1: $F_{1,519} = 0.8$, $p = 0.3$). Including all wind directions, attenuation by the reefs was significantly higher compared to the control with water levels below 0.5 m, but not with higher water levels (two-way ANOVA: $F_{2,\ 1719} = 283.4$, $p < 0.001$ [effect of the treatment]) (Figs. A.1 and A.2a). When analysing the wave attenuation data from only days with winds perpendicular to the set-up (130 to 190 degrees, therefore reef and control subjected to the same waves coming offshore), the results were the same but the variability was reduced, confirming the effect of the reef (two-way ANOVA: $F_{2,\ 132} = 28.9$, $p < 0.001$ [effect of the treatment]) (Fig. A.2b). The highest variability in wave attenuation therefore occurred during tides with winds coming from directions not perpendicular to the set-up, primarily from the south west (200–300 degrees), which were lateral to the experimental set-up (Fig. 3). In addition, these south west winds had the highest wind speeds and were related to higher mean water depth and significant wave height, therefore, related to less wave attenuation by the artificial reefs (Fig. A.3).

The mean attenuation by the artificial reef started to decrease below 30% after September 2017 due to the reef degradation and was absent from September 2017 onwards (ANCOVA for period 2: $F_{1,310} = 0.7$, $p = 0.37$; and period 3: $F_{1,208} = 0.03$, $p = 0.84$) (Fig. 2b,c).

3.2. Effect of the artificial reefs on sediment dynamics

Due to the high exposure of the study site and the migrating large bedforms, there were strong and complex large-scale sediment dynamics in the experimental area (Fig. 4). The effect of the artificial reefs on sediment dynamics did not expand beyond 10 m from the landward edge of the structures and varied between plots. The migration of natural bedforms, unrelated to the experiment, interfered with the measurement of changes in bed level caused by the artificial structures, however the effect of the reefs was still visible (Fig. A.4). The magnitude of these effects can best be seen in the changes in bed level in the control plots. Satellite images of these migrating bedforms between 2017 and 2019 can be found in Fig. A.5.

At the local scale (plots of 20 × 10 m, Fig. 1), both sediment trapping and scouring often occurred simultaneously within a single plot (Fig. 4 and 5a,b,c). Overall, most of the reefs significantly increased the maximum elevation locally up to 11 cm compared to the controls, independently of time and block (3-way ANOVA: $F_{1,30} = 27.86$, $p < 0.001$). However, the first two reef plots always accreted less due to the large bedforms unrelated to the experiment (Fig. 4 and 5b). At the same time, some reefs also induced higher scouring than the control plots (3-

Table 1
Mean cumulative degradation of the artificial reefs height over time (±SD), with respect to the initial installed height (~ 20 cm).

	May 2017	August 2017	August 2018	August 2019
	($n = 16$)	(n = 16)	(n = 16)	(n = 16)
Mean cumulative artificial reef height degradation (cm)	0.0 ± 2.4	0.0 ± 2.2	−12.6 ± 2.5	−14 ± 1.9
Remaining reef height (cm)	~20 (intact)	~20 (intact)	~8 (degraded)	~6 (degraded)

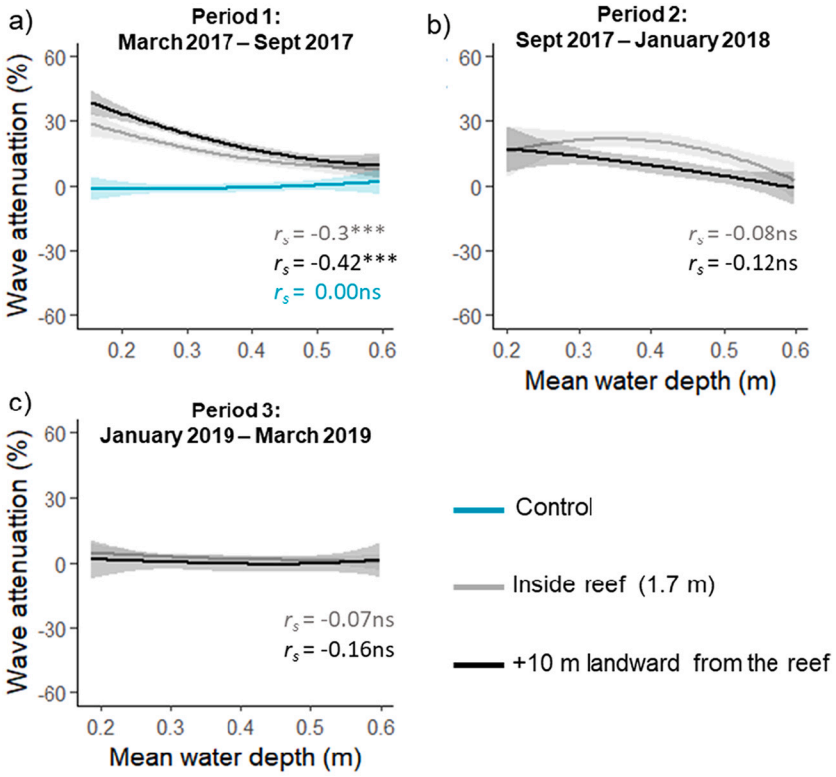

Fig. 2. Wave attenuation by the artificial reef compared to the bare tidal flat (control) including all the wind directions during a) March 2017 to August 2017, with intact reef, b) September 2017 to January 2018, with the reef starting to degrade and the control sensor lost, and c) January 2019 to March 2019, with degraded and buried reef and control sensor lost. The mean water depth is only shown until 0.6 m, where the effect of the reefs was negligible. Significant codes refer to $p < 0.001$ (***) and $p > 0.05$ (ns).

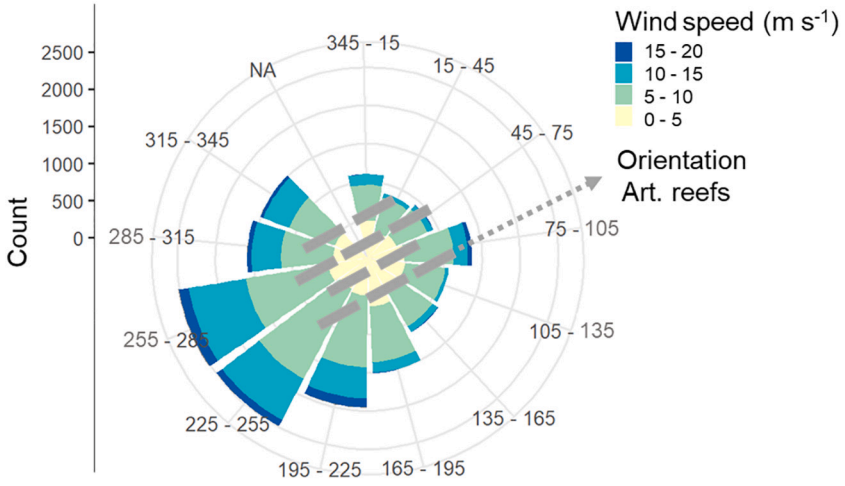

Fig. 3. Wind speed and wind directions during the experimental period. The grey blocks indicate the position of the artificial reef modules with respect to the north and how they were parallelly exposed to the predominant wind direction (200–300 degrees). Frequency of each wind type (combination of wind direction and wind speed) are represented as count in the length of the bins.

way ANOVA: $F_{1,30} = 9.1$, $p = 0.004$) (Fig. 5b,c), leading to more variable elevation within each reef plot (3-way ANOVA: $F_{1,30} = 28.6$, $p < 0.001$) (Fig. 5d). Due to the balance between eroding and accreting zones within each single plot and the first two reefs which had more erosion, the overall effect of the reefs on the net accretion at the local scale during all the experimental period did not significantly differ from the controls (3-way ANOVA: $F_{1,30} = 1.89$, $p = 0.17$) (Fig. 5e).

In May 2017, the maximum accretion within reefs was 6 cm compared to the 3 cm in the control plots, while the net accretion was ~0 cm for both treatments. In August 2017, the net sedimentation was negative (~ −4 to ~−2 cm), while the maximum accretion within the reefs was 5 cm and 4 cm in the controls. In August 2018, mean net accretion was around 0 cm, and although the structures started to degrade, sediment was still trapped by the reefs up to 11 cm, with the highest sediment accretion occurring in the five centre-most reef plots. The sedimentation pattern of the artificial reefs was related to the migrating bedforms, with higher sediment deposition in the areas where the crest of the bedforms encountered a reef (Fig. 4, Figs. A.4 and A.5). Lastly, in August 2019, when the artificial reefs were in their most degraded state, mean neat accretion was around 0 cm in the reefs and –3 cm in the controls. However, sediment accretion up to 6 cm was still present in the five centre-most reef plots, compared to a maximum of 3 cm in the controls (Figs. 4, 5b, and Fig. A.4).

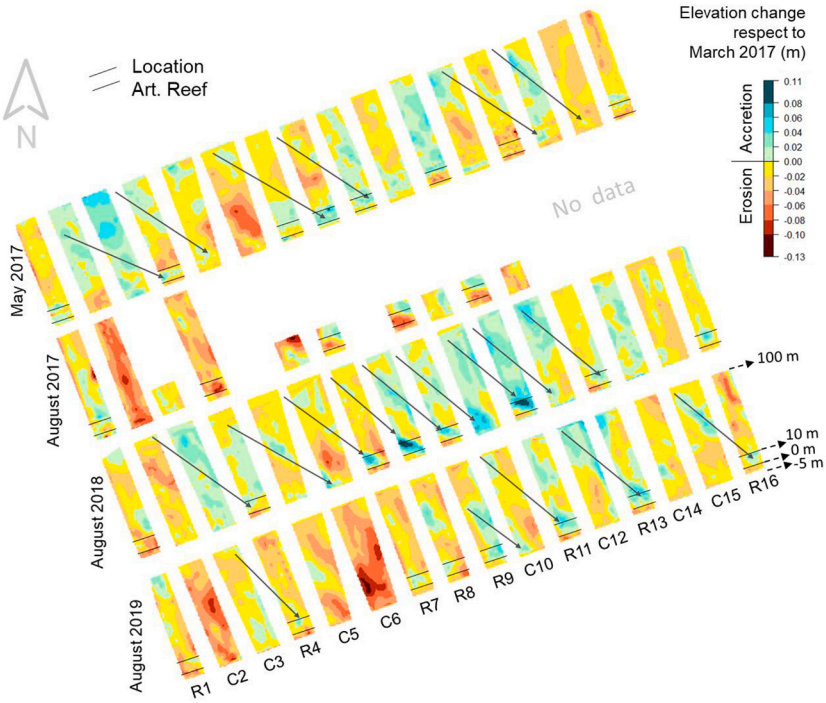

Fig. 4. Digital elevation models (DEM) of the 105 m transects showing the elevation changes for each time period compared to the initial elevation in March 2017. Arrows indicate the direction of the crest of some of the large bedforms and black lines the location of the artificial reefs. During the whole experimental period, there were areas with up to 13 cm of erosion (dark red areas) and areas with up to 11 cm accretion (dark green areas). (For interpretation of the references to colour in this figure legend, the reader is referred to the web version of this article.)

3.3. Effect of artificial reefs on sediment properties

Overall, sediment properties did not significantly differ between control and artificial reef plots [$X^2(1) = 0.003$, $p = 0.95$ (mean grain size), $X^2(1) = 0.21$, $p = 0.64$ (silt %), $X^2(1) = 1.57$, $p = 0.21$ (organic matter %)] (Fig. A.6). Variability in these properties was mainly found over time. Mean grain size ranged from 180 to 240 μm and overall smaller grain sizes were found in August 2017 ($X^2(3) = 38.74$, $p < 0.001$). Silt % ranged from 0 to 6.5%, being lower in August 2017 ($X^2(3) = 53.22$, $p < 0.001$). Organic matter ranged from 0.6 to 1.18% and was significantly lower in August 2017 ($X^2(3) = 153.01$, $p < 0.001$).

4. Discussion

Ecosystem-based or nature-based coastal defence provides a promising coastal protection framework (Temmerman et al., 2013; Schoonees et al., 2019). Hence, there is need for understanding how we can use low-intertidal tidal flat ecosystems to stabilize wave-attenuating high intertidal coastal systems, by making use of cross-habitat connectivity. Our study is the first of its kind to experimentally test the potential of biodegradable artificial reefs for foreshore coastal protection through tidal-flat stabilization. In this study, we tested the use of a 630 m long biodegradable artificial reefs for attenuating waves and stabilizing and accreting sediment on a tidal flat, as alternative to hard engineering structures typically used for this purpose (Schoonees et al., 2019). We showed that the artificial reefs could reduce wave heights up to 60% and on average 30%, compared to the adjacent bare tidal flat, despite being placed in a highly exposed area. Interestingly, we discovered that artificial reef effects on local sediment dynamics interfered with migrating bedforms, as result of the scale of our experiment. However, it was still clear that biodegradable reefs were able to accrete sediment at a local scale, depending on the time the ephemeral reefs persisted. In addition, surrounding sediment properties were not affected by the presences of the structures. The use of biodegradable artificial reefs looks promising for local and temporal tidal flat stabilization due to wave attenuation and sediment trapping, but promoting large-scale connectivity between tidal flats and high intertidal systems such as salt marsh would require a much larger spatial scale than our current experiment.

4.1. Wave attenuation by biodegradable artificial reefs and interaction with wind conditions

The ratio of water depth to structure height is an important variable for wave attenuation. The higher the water levels relative to the structure height, the less attenuation will occur (Möller et al., 1999; Ysebaert et al., 2011; Yang et al., 2012; Chowdhury et al., 2019). In our experiment, waves were attenuated mainly during the first measurement period (March 2017 to August 2017) when artificial reefs were still ~20 cm high and only when water levels were below 0.5 m. Wave attenuation by vegetation or reefs also depends on the relative wave height (significant wave height relative to the water depth, H_s/h) (Möller, 2006; Ysebaert et al., 2011; Yang et al., 2012; Donker et al., 2013). In our study, small values of H_s/h (< 0.2) led to less attenuation because either the water was too deep or the waves too small to interact with the reefs. In contrast, high values of H_s/h (>0.4) which can lead to wave breaking were also less attenuated (Kroon, 1994; Donker et al., 2013). Lastly, in our study, an increase in attenuation variability appeared when strong winds were coming from the south west, which led to higher water levels and wave heights. In addition, these winds were parallel to the set-up; instead of perpendicular, which obviously greatly reduce the efficiency of wave attenuation. Overall, this indicates that the orientation of the structures relative to the wind direction may determine their wave attenuating and thus stabilizing effects. However, as our experiment was near an island, the wind conditions pushing waves over the reef can vary much more widely compared to a much wider mainland foreshore.

4.2. Effect of the biodegradable artificial reefs on tidal flat sediment dynamics

The installation of stiff structures in a tidal flat can lead to sediment erosion and accretion patterns within the structures and in the near surroundings (Bouma et al., 2007, 2009; Walles et al., 2015). In our study, the installation of artificial reefs in the tidal flat also led to both erosion (up to −11 cm) and accretion (up to +11 cm) at the local scale (~ 10 m landwards from the reef). Interestingly, the sedimentation pattern of the artificial reefs was related to the migrating large bedforms,

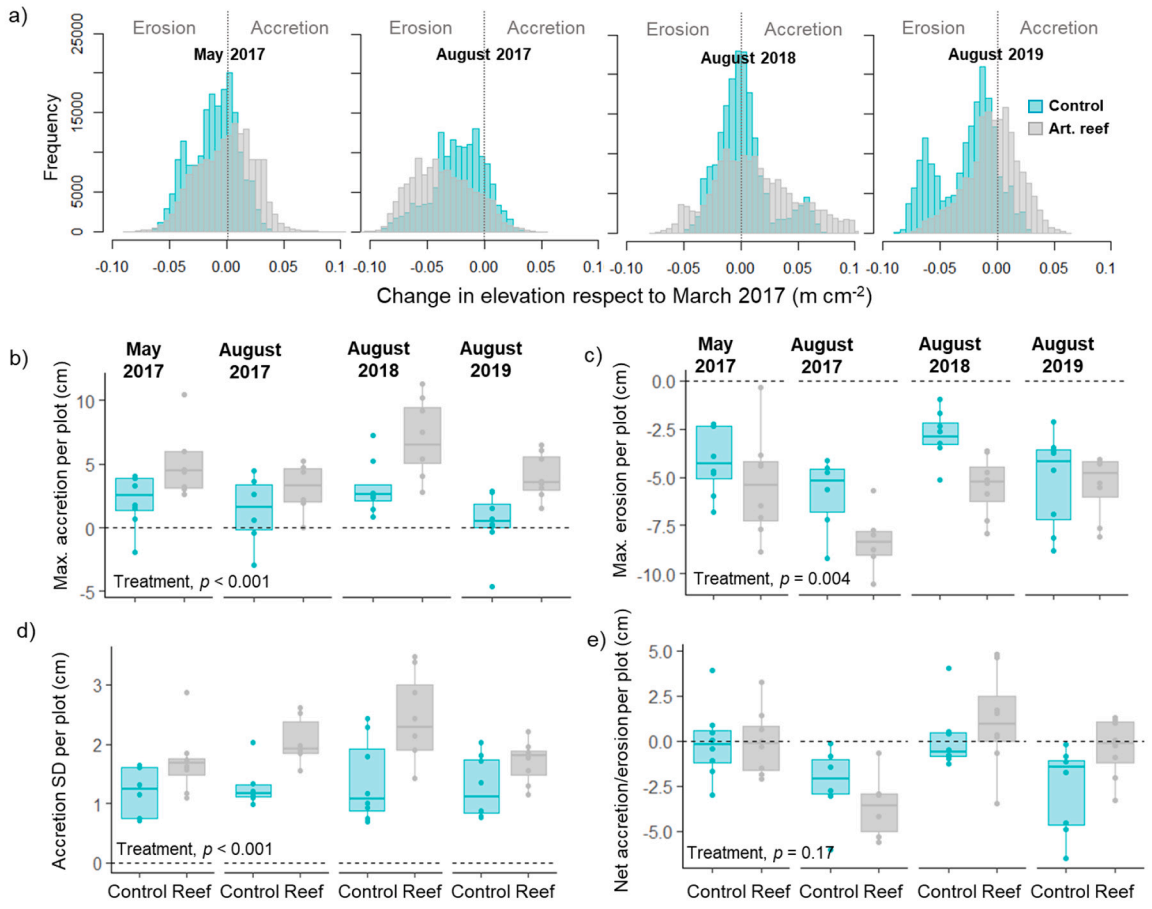

Fig. 5. a) Distributions of the elevation changes (m) per pixel (1 cm^2) in control and artificial reefs plots at a local scale (plot of 10 × 20 m); and boxplots of the b) maximum accretion per plot (cm), c) maximum erosion per plot (cm), d) standard deviation of the accretion per plot (cm) and e)net accretion/erosion per plot (cm), all at a local scale and separated by treatment and time-step. *P* values correspond to 3-way ANOVAs.

with higher sediment deposition in the areas where the crest of the bedforms encountered a reef (Figs. A.4 and A.5). This accretion was more evident in August 2018 and mainly in the landward side of the structures. In contrast, in August 2017, when the structures were still intact, more sediment scouring and erosion was observed. This suggest that whereas higher structures can lead to higher wave attenuation, it can also lead to higher sediment scouring due to enhanced turbulences.

Migrating bedforms have been found in different areas of upper tidal flats in the Wadden Sea, and are influenced by the tidal dynamics (Donker et al., 2013; Adolph et al., 2018). These migrating bedforms led to values of sediment accretion in control plots in this study. However, the maximum sedimentation in the reefs plots was still higher compared to controls, confirming their effect on sediment accretion. This sedimentation in the field can be visualized in the Fig. A.4. Nevertheless, the net accretion, taking into account all areas that eroded and accreted, was always similar in reef and control plots. Sediment could be trapped due to the wave attenuation effect, but likely due to flow attenuation (Bouma et al., 2007, 2009; Donadi et al., 2013; Colden et al., 2016) as observed in August 2019 when the reefs were degraded thus not attenuating waves but still accreting sediment compared to the control plots. This indicates that although ~6 cm high reefs did not affect wave attenuation, they likely affected the sediment dynamics by attenuating the water flow. Flow attenuation and subsequent sediment trapping by this type of artificial reefs has been demonstrated in a flow flume experiment, where flow velocities were attenuated by an order of magnitude compared to a bare treatment (from 8.5, 14.5, and 23 cm/s to 0.7, 1.6, and 2.5 cm/s) over the first 50 cm of a 6 cm high BESE structure (Fivash et al., 2021).

4.3. *Effect of the biodegradable artificial reefs on sediment properties*

Natural shellfish reefs can change their environmental surrounding, both biotic and abiotically by creating calm conditions and/or by their faeces and pseudo-faeces (Donadi et al., 2013, 2015; Salvador de Paiva et al., 2018). By installing artificial reefs, we were expecting an increase in organic matter or fine sediments by the creation of calmer conditions and by the possible mussel establishment on the reefs which could produce faeces and pseudo-faeces (Donadi et al., 2015; Chowdhury et al., 2019). However, although sedimentation was observed and mussel establishment occurred (Temmink, 2020), the artificial reefs did not have an overall significant effect on sediment properties compared to the control plots . This may be due to the high exposure of the site, which did not let to settle changes in the sediment properties or because higher mussel densities during a longer period were needed to observe a significant effect (Temmink, 2020).

4.4. *Application of biodegradable artificial reefs for coastal protection*

The results of this study on the effect of biodegradable artificial reefs on tidal flat stabilization together with the mussel establishment observed (Temmink, 2020), emphasizes the importance of distinguishing the application of these structures depending on the aim: ecological

(i. e. mussel bed restoration) or engineering (i. e. stabilization of the tidal flat) as previously pointed out by Morris et al. (2019). Mussel bed restoration is sensitive to strong hydrodynamics (De Paoli et al., 2015; Schotanus et al., 2020), and often it is exactly at these locations where management for coastal protection is needed. In addition, the effect of the artificial reefs on trapping sediment, which is desired for coastal protection, may counteract the mussel establishment (Walles et al., 2016b; Temmink, 2020).

Overall, our set-up was not sufficiently resistant to persist long term, or to sustain a stable mussel reef which would overtake the effect of the artificial reefs on trapping sediment. Moreover, the set-up was not large enough to have a significant large scale effect in the tidal flat morphology. If the aim is solely to restore mussel beds using biodegradable artificial reefs, a more sheltered location may be preferred (Piazza et al., 2005). In the other hand, if the aim is to integrate ecosystem restoration as part of a coastal protection scheme, aimed at long-term tidal flat stabilization at an exposed location, it would be recommended to use a large set-up with more resistant material. For example, one should build wider and longer structures as well as dispose the blocks along the foreshore but also across the foreshore. This would help to attenuate hydrodynamics in a bigger area and therefore have a larger effect on sediment stabilization (Walles et al., 2015). The width of the bedforms occurring at the tidal flat could be a good starting point to design the length of each reef plot. For example, in our system this could be between 10 and 30 m, which is similar to the length of the natural bed-forms. Also, the installation of more bands of reefs going landwards and perpendicular to the bedforms or flow direction could create sedimentation in a larger area (Colden et al., 2016). The orientation facing the tidal flow direction may be the most effective for sediment trapping because as seen in this study, even when not reducing waves due to the degradation of the structures height, the could still trap sediment likely due to flow attenuation. If using higher structures, a test of the resistance of the material and effect on sediment dynamics should be done because this could increase scouring. Lastly, installing the reefs higher in the tidal flat could have a greater impact on the marsh, but the feasibility of it on developing on a mussel bed will depend on the tidal range and flood frequency of the location for the biogenic reef establishment and survival (Walles et al., 2016a).

Credit author statement

B.M.-D., G.S.F., J.N., R.J.M.T., V.C.R, K.D, J.T.H,E.P., J.v.B., M.J.A.C., T.v.d.H., D.v.d.W., H.O., T.J.B. and L.L.G. conceived the ideas and designed the methodology; B.M.-D., G.S.F., J.N., RJ.M.T., N.H., V.C.R., P.P.M.J.M.C., K.D., J.T.H,E.P., G.M.-G., M.J.A.C., T.v.d.H., T.J.B. and L.L.G. collected the data; B.M.-D. analysed the data; G.S.F, J.v.B., J.C.d.S and H.O. contributed to the data analysis; B.M.-D. led the writing of the manuscript. All authors contributed critically to the drafts and gave final approval for publication.

Declaration of Competing Interest

The authors declare that they have no known competing financial interests or personal relationships that could have appeared to influence the work reported in this paper.

Acknowledgements

This work is part of the Perspectief research programme All-Risk with project number P15-21 project B1 which is (partly) financed by NWO Domain Applied and Engineering Sciences, in collaboration with the following private and public partners: the Dutch Ministry of Infrastructure and Water Management (RWS), Deltares, STOWA, the regional water authority Noorderzijlvest, the regional water authority Vechtstromen, it Fryske Gea, HKV consultants, Natuurmonumenten, waterboard HHNK. LLG was supported by NWO-VENI grant 016. VENI.181.087. H.O., E.P and L.L.G were funded by Waddenfonds and Rijkswaterstaat, for the project 'dynamic Griend'. T.v.d.H, L.L.G and V. C.R. were additionally funded by OBN. R.J.M.T., G.S.F. and K.D. were funded by NWO/TTW-OTP grant 14424, in collaboration with private and public partners: Natuurmonumenten, STOWA, Rijkswaterstaat, Van Oord, Bureau Waardenburg, Enexio and Rodenburg Biopolymers. T.v.d. H. was funded by NWO/TTW-Vidi grant 16588. In addition, we would like to thank the anonymous reviewers for their constructive comments in the previous version of this manuscript, to all volunteers who helped with setting up and monitoring the experiments, to Sien, Saar and Jouke who have hosted us on the Ambulant and to the crew of the Asterias from the 'Wadden Unit' for enabling transport to and from the experiment. The authors declare no conflict of interest.

Appendix A. Supplementary data

Supplementary data to this article can be found online at https://doi.org/10.1016/j.ecoleng.2021.106354.

References

Adolph, W., Farke, H., Lehner, S., Ehlers, M., 2018. Remote sensing intertidal flats with TerraSAR-X.A SAR perspective of the structural elements of a tidal basin for monitoring the Wadden Sea. Remote Sens. 10 https://doi.org/10.3390/rs10071085.

Barbier, E.B., Hacker, S.D., Kennedy, C., Kock, E.W., Stier, A.C., Brian, R.S., 2011. The value of estuarine and coastal ecosystem services. Ecol. Monogr. 81, 169–193. https://doi.org/10.1890/10-1510.1.

Bates, D., Mächler, M., Bolker, B.M., Walker, S.C., 2015. Fitting linear mixed-effects models using lme4. J. Stat. Softw. 67 (1), 1–48. https://doi.org/10.18637/jss.v067.i01.

Bishop, M.J., Mayer-Pinto, M., Airoldi, L., et al., 2017. Effects of ocean sprawl on ecological connectivity: impacts and solutions. J. Exp. Mar. Biol. Ecol. 492, 7–30. https://doi.org/10.1016/j.jembe.2017.01.021.

Borsje, B.W., van Wesenbeeck, B.K., Dekker, F., Paalvast, P., Bouma, T.J., van Katwijk, M.M., de Vries, M.B., 2011. How ecological engineering can serve in coastal protection. Ecol. Eng. 37, 113–122. https://doi.org/10.1016/j.ecoleng.2010.11.027.

Bos, A.R., Bouma, T.J., de Kort, G.L.J., van Katwijk, M.M., 2007. Ecosystem engineering by annual intertidal seagrass beds: Sediment accretion and modification. Estuar. Coast. Shelf Sci. 74, 344–348. https://doi.org/10.1016/j.ecss.2007.04.006.

Bouma, T.J., van Duren, L.A., Temmerman, S., Claverie, T., Blanco-Garcia, A., Ysebaert, T., Herman, P.M.J., 2007. Spatial flow and sedimentation patterns within patches of epibenthic structures: combining field, flume and modelling experiments. Cont. Shelf Res. 27, 1020–1045. https://doi.org/10.1016/j.csr.2005.12.019.

Bouma, T.J., Friedrichs, M., Van Wesenbeeck, B.K., Temmerman, S., Graf, G., Herman, P. M.J., 2009. Density-dependent linkage of scale-dependent feedbacks : a flume study on the intertidal macrophyte Spartina anglica. Oikos 118, 260–268. https://doi.org/10.1111/j.1600-0706.2008.16892.x.

Bouma, T.J., van Belzen, J., Balke, T., et al., 2014. Identifying knowledge gaps hampering application of intertidal habitats in coastal protection: opportunities & steps to take. Coast. Eng. 87, 147–157. https://doi.org/10.1016/j.coastaleng.2013.11.014.

Bouma, T.J., van Belzen, J., Balke, T., et al., 2016. Short-term mudflat dynamics drive long-term cyclic salt marsh dynamics. Limnol. Oceanogr. 61, 2261–2275. https://doi.org/10.1002/lno.10374.

Chowdhury, M.S.N., Walles, B., Sharifuzzaman, S., Shahadat Hossain, M., Ysebaert, T., Smaal, A.C., 2019. Oyster breakwater reefs promote adjacent mudflat stability and salt marsh growth in a monsoon dominated subtropical coast. Sci. Rep. 9 https://doi.org/10.1038/s41598-019-44925-6.

Christianen, M.J.A., van Belzen, J., Herman, P.M.J., van Katwijk, M.M., Lamers, L.P.M., van Leent, P.J.M., Bouma, T.J., 2013. Low-canopy seagrass beds still provide important coastal protection services. PLoS One 8. https://doi.org/10.1371/journal.pone.0062413.

Christianen, M.J.A., van der Heide, T., Holthuijsen, S.J., van der Reijden, K.J., Borst, A.C. W., Olff, H., 2017. Biodiversity and food web indicators of community recovery in intertidal shellfish reefs. Biol. Conserv. 213, 317–324. https://doi.org/10.1016/j.biocon.2016.09.028.

Colden, A.M., Fall, K.A., Cartwright, G.M., Friedrichs, C.T., 2016. Sediment suspension and deposition across restored oyster reefs of varying orientation to flow: implications for restoration. Estuar. Coasts 39, 1435–1448. https://doi.org/10.1007/s12237-016-0096-y.

De Paoli, H., Van De Koppel, J., Van Der Zee, E., Kangeri, A., Van Belzen, J., 2015. Processes limiting mussel bed restoration in the Wadden-Sea. J. Sea Res. 103, 42–49. https://doi.org/10.1016/j.seares.2015.05.008.

R Development Core Team (2018). R: A language and environment for statistical computing. Retrieved from https://www.r-project.org/.

Donadi, S., van der Heide, T., van der Zee, E.M., et al., 2013. Cross-habitat Interactions Among Bivalve Species Control Community Structure on Intertidal Flats, 94, pp. 489–498.

Donadi, S., van der Heide, T., Piersma, T., et al., 2015. Multi-scale Habitat Modification by Coexisting Ecosystem Engineers Drives Spatial Separation of Macrobenthic Functional Groups, pp. 1502–1510. https://doi.org/10.1111/oik.02100.
Donker, J.J.A., Van Der Vegt, M., Hoekstra, P., 2013. Wave forcing over an intertidal mussel bed. J. Sea Res. 82, 54–66. https://doi.org/10.1016/j.seares.2012.08.010.
Doody, J.P., 2013. Coastal squeeze and managed realignment in southeast England , does it tell us anything about the future ? Ocean Coast. Manag. 79, 34–41. https://doi.org/10.1016/j.ocecoaman.2012.05.008.
Fivash, G.S., van Belzen, J., Temmink, R.J.M., Didderen, K., Lengkeek, W., van der Heide, T., Bouma, T.J., 2020. Elevated micro-topography boosts growth rates in Salicornia procumbens by amplifying a tidally driven oxygen pump: implications for natural recruitment and restoration. Ann. Bot. 125, 353–364. https://doi.org/10.1093/aob/mcz137.
Fivash, G.S., Temmink, R.J.M., D'Angelo, M., et al., 2021. Restoration of biogeomorphic systems by creating windows of opportunity to support natural establishment processes. Ecol. Appl. 0, 1–16. https://doi.org/10.1002/eap.2333.
Folmer, E., Büttger, H., Herlyn, M., Markert, A., Millat, G., Troost, K., Wehrmann, A., 2017. Beds of blue mussels and Pacific oysters. In: Wadden Sea Quality Status Report 2017. Common Wadden Sea Secretariat.
Fonseca, M.S., Cahalan, J.A., 1992. A preliminary evaluation of wave attenuation by four species of seagrass. Estuar. Coast. Shelf Sci. 35, 565–576. https://doi.org/10.1016/S0272-7714(05)80039-3.
Gillis, L.G., Bouma, T.J., Jones, C.G., Van Katwijk, M.M., Nagelkerken, I., Jeuken, C.J.L., Herman, P.M.J., Ziegler, A.D., 2014. Potential for landscape-scale positive interactions among tropical marine ecosystems. Mar. Ecol. Prog. Ser. 503, 289–303. https://doi.org/10.3354/meps10716.
Hu, Z., Van Belzen, J., Van Der Wal, D., Balke, T., Wang, Z.B., Stive, M., Bouma, T.J., 2015. Windows of opportunity for salt marsh vegetation establishment on bare tidal flats: the importance of temporal and spatial variability in hydrodynamic forcing. J. Geophys. Res. G Biogeosci. 120, 1450–1469. https://doi.org/10.1002/2014JG002870.
Kroon, A., 1994. Sediment Transport and Morphodynamics of the Beach and Nearshore Zone Near Egmond. University of Utrecht, The Netherlands.
Ladd, C.J.T., Duggan-Edwards, M.F., Bouma, T.J., Pagès, J.F., Skov, M.W., 2019. Sediment supply explains long-term and large-scale patterns in salt marsh lateral expansion and erosion. Geophys. Res. Lett. 46, 11178–11187. https://doi.org/10.1029/2019GL083315.
Marin-Diaz, B., Bouma, T.J., Infantes, E., 2019. Role of eelgrass on bed-load transport and sediment resuspension under oscillatory flow. Limnol. Oceanogr. 426–436 https://doi.org/10.1002/lno.11312.
Mariotti, G., Fagherazzi, S., 2013. Critical width of tidal flats triggers marsh collapse in the absence of sea-level rise. Proc. Natl. Acad. Sci. 110, 5353–5356. https://doi.org/10.1073/pnas.1219600110.
Meyer, D.L., Townsend, E.C., Thayer, G.W., 1997. Erosion Control Value of Oyster Cultch for Intertidal Marsh, 5, pp. 93–99.
Möller, I., 2006. Quantifying saltmarsh vegetation and its effect on wave height dissipation: results from a UK East coast saltmarsh. Estuar. Coast. Shelf Sci. 69, 337–351. https://doi.org/10.1016/j.ecss.2006.05.003.
Möller, I., Spencer, T., French, J.R., Leggett, D.J., Dixon, M., 1999. Wave transformation over salt marshes : a field and numerical modelling study from North Norfolk, England. Estuar. Coast. Shelf Sci. 411–426.
Möller, I., Kudella, M., Rupprecht, F., et al., 2014. Wave attenuation over coastal salt marshes under storm surge conditions. Nat. Geosci. 7 https://doi.org/10.1038/ngeo2251.
Morris, R.L., Konlechner, T.M., Ghisalberti, Swearer, S.E., 2018. From grey to green: efficacy of eco-engineering solutions for nature-based coastal defence. Glob. Chang. Biol. 1827–1842. https://doi.org/10.1111/gcb.14063.
Morris, R.L., Bilkovic, D.M., Boswell, M.K., et al., 2019. The application of oyster reefs in shoreline protection: are we over-engineering for an ecosystem engineer? J. Appl. Ecol. 56, 1703–1711. https://doi.org/10.1111/1365-2664.13390.
Murray, N.J., Phinn, S.R., DeWitt, M., et al., 2019. The global distribution and trajectory of tidal flats. Nature 565, 222–225. https://doi.org/10.1038/s41586-018-0805-8.
Piazza, B.P., Banks, P.D., La Peyre, M.K., 2005. The potential for created oyster shell reefs as a sustainable shoreline protection strategy in Louisiana. Restor. Ecol. 13, 499–506. https://doi.org/10.1111/j.1526-100X.2005.00062.x.
RWS, 2013. Kenmerkende waarden. Getijgebied 2011.0.
Salvador de Paiva, J.N., Walles, B., Ysebaert, T., Bouma, T.J., 2018. Understanding the conditionality of ecosystem services : the effect of tidal flat morphology and oyster reef characteristics on sediment stabilization by oyster reefs. Ecol. Eng. 112, 89–95. https://doi.org/10.1016/j.ecoleng.2017.12.020.
Schoonees, T., Gijón Mancheño, A., Scheres, B., Bouma, T.J., Silva, R., Schlurmann, T., Schüttrumpf, H., 2019. Hard structures for coastal protection, towards greener designs. Estuar. Coasts 42, 1709–1729. https://doi.org/10.1007/s12237-019-00551-z.
Schotanus, J., Capelle, J.J., Paree, E., Fivash, G.S., van de Koppel, J., Bouma, T.J., 2020. Restoring mussel beds in highly dynamic environments by lowering environmental stressors. Restor. Ecol. 1–11. https://doi.org/10.1111/rec.13168.
Shepard, C.C., Crain, C.M., Beck, M.W., 2011. The protective role of coastal marshes: a systematic review and meta-analysis. PLoS One 6. https://doi.org/10.1371/journal.pone.0027374.
Siemes, R.W.A., Borsje, B.W., Daggenvoorde, R.J., Hulscher, S.J.M.H., 2020. Artificial structures steer morphological development of salt marshes: a model study. J. Mar. Sci. Eng. 8 https://doi.org/10.3390/JMSE8050326.
Temmerman, S., Meire, P., Bouma, T.J., Herman, P.M.J., Ysebaert, T., De Vriend, H.J., 2013. Ecosystem-based coastal defence in the face of global change. Nature 504, 79–83. https://doi.org/10.1038/nature12859.
Temmink, R.J.M., 2020. The Restoration of Wetlands Dominated by Habitat Modifiers. PhD Thesis. University of Groningen. https://repository.ubn.ru.nl/handle/2066/225923.
Temmink, R.J.M., Christianen, M.J.A., Fivash, G.S., et al., 2020. Mimicry of emergent traits amplifies coastal restoration success. Nat. Commun. 1–9 https://doi.org/10.1038/s41467-020-17438-4.
van de Koppel, J., van der Heide, T., Altieri, A.H., Eriksson, B.K., Bouma, T.J., Olff, H., Silliman, B.R., 2015. Long-distance interactions regulate the structure and resilience of coastal ecosystems. Annu. Rev. Mar. Sci. 7, 139–158. https://doi.org/10.1146/annurev-marine-010814-015805.
Van Loon-steensma, J.M., Slim, P.A., 2013. The impact of erosion protection by stone dams on salt-marsh vegetation on two wadden sea barrier islands stable. URL : http://www.jstor.org/stable/23486550 linked references are available on JSTOR for this article : the impact of erosion protection by Sto. J. Coast. Res. 29, 783–796.
Walles, B., Salvador de Paiva, J., van Prooijen, B.C., Ysebaert, T., Smaal, A.C., 2015. The ecosystem engineer crassostrea gigas affects tidal flat morphology beyond the boundary of their reef structures. Estuar. Coasts 38, 941–950. https://doi.org/10.1007/s12237-014-9860-z.
Walles, B., Fodrie, F.J., Nieuwhof, S., Jewell, O.J.D., Herman, P.M.J., Ysebaert, T., 2016a. Guidelines for evaluating performance of oyster habitat restoration should include tidal emersion: reply to Baggett et al. Restor. Ecol. 24, 4–7. https://doi.org/10.1111/rec.12328.
Walles, B., Troost, K., van den Ende, D., Nieuwhof, S., Smaal, A.C., Ysebaert, T., 2016b. From artificial structures to self-sustaining oyster reefs. J. Sea Res. 108, 1–9. https://doi.org/10.1016/j.seares.2015.11.007.
Willemsen, P.W.J.M., Borsje, B.W., Hulscher, S.J.M.H., et al., 2017. Quantifying bed level change at the transition of tidal flat and salt marsh : can we understand the lateral location of the marsh edge ? J. Geophys. Res. Earth Surf. 2509–2524. https://doi.org/10.1029/2018JF004742.
Willemsen, P.W.J.M., Borsje, B.W., Vuik, V., Bouma, T.J., Hulscher, S.J.M.H., 2020. Field-based decadal wave attenuating capacity of combined tidal flats and salt marshes field-based decadal wave attenuating capacity of combined tidal flats and salt marshes. Coast. Eng. 156, 103628. https://doi.org/10.1016/j.coastaleng.2019.103628.
Yang, S.L., Shi, B.W., Bouma, T.J., Ysebaert, T., Luo, X.X., 2012. Wave attenuation at a salt marsh margin: a case study of an exposed coast on the Yangtze Estuary. Estuar. Coasts 35, 169–182. https://doi.org/10.1007/s12237-011-9424-4.
Ysebaert, T., Yang, S.L., Zhang, L., He, Q., Bouma, T.J., Herman, P.M.J., 2011. Wave attenuation by two contrasting ecosystem engineering salt marsh macrophytes in the intertidal pioneer zone. Wetlands 31, 1043–1054. https://doi.org/10.1007/s13157-011-0240-1.
Zhu, Z., Vuik, V., Visser, P.J., et al., 2020. Historic storms and the hidden value of coastal wetlands for nature-based flood defence. Nat. Sustain. 3, 853–862. https://doi.org/10.1038/s41893-020-0556-z.